

# Learning from Small Samples: Transformation-Invariant SVMs with Composition and Locality at Multiple Scales

Tao Liu, P. R. Kumar, Ruida Zhou, and Xi Liu

Texas A&M University

Email: {tliu, prk, ruida, xiliu}@tamu.edu

**Abstract**—Motivated by the problem of learning with small sample size, this paper shows how to incorporate into support-vector machines (SVMs) those properties that have made convolutional neural networks (CNNs) successful. Particularly important is the ability to incorporate domain knowledge of invariances, e.g., translational invariance of images. Kernels based on the *maximum* similarity over a group of transformations are not generally positive definite. Perhaps it is for this reason that they have neither previously been experimentally tested for their performance nor studied theoretically. We address this lacuna and show that positive definiteness indeed holds *with high probability* for kernels based on the maximum similarity in the small training sample set regime of interest, and that they do yield the best results in that regime. We also show how additional properties such as their ability to incorporate local features at multiple spatial scales, e.g., as done in CNNs through max pooling, and to provide the benefits of composition through the architecture of multiple layers, can also be embedded into SVMs. We verify through experiments on widely available image sets that the resulting SVMs do provide superior accuracy in comparison to well-established deep neural network benchmarks for small sample sizes.

## I. INTRODUCTION

With the goal of learning when the number of training samples is small, and motivated by the success of CNNs [29], [25], we wish to endow SVMs with as much a priori domain knowledge as possible.

One such important domain property for image recognition is translational invariance. An image of a dog remains an image of the same dog if the image is shifted to the left. Similarly, if the image is rotated it is still an image of the dog; so it is also rotation-invariant. More generally, given a group of transformations under which the classification of images is invariant, we show how to endow SVMs with the knowledge of such invariance.

One common approach is data augmentation [22], [6], where several transformations of each training sample are added to the training set. When applying SVMs on this augmented training set, it corresponds to a kernel that defines the similarity between two vectors  $X_1$  and  $X_2$  as the *average similarity* between  $X_1$  and all transformations of  $X_2$ . However the average also includes transformations that are maximally dissimilar, and we show that it leads to poor margins and poor classification results. More appealing is to define a kernel that defines similarity as the *greatest similarity* between  $X_1$

and all transformations of  $X_2$ . We show that this kernel is positive definite with high probability in the small sample regime of interest to us, under a probabilistic model for features. We verify this property on widely available datasets and show that the improvement obtained by endowing SVMs with this transformation invariance yields considerably better test accuracy.

Another important domain property for image recognition is the “locality” of features, e.g., an edge depends only on a sharp gradient between neighboring pixels. Through operations such as max-pooling, CNNs exploit locality at multiple spatial scales. We show how one may incorporate such locality into polynomial SVMs.

Finally, their multi-layer architecture provides CNNs the benefits of composition [7]. We show how one can iteratively introduce multiple layers into SVMs to facilitate composition. The introduction of multiple layers increases computational complexity, and we show how this can be alleviated by parallel computation so as to achieve a reduction of computation time by increasing memory.

We show experimentally that the resulting SVMs provide significantly improved performance for small datasets. Translational and rotational invariance embedded into SVMs allows them to recognize objects that have not already been centered in images or oriented in upright positions; we refer to these as transformed datasets in the sequel. The transformation-invariant SVMs provide significant improvements over SVMs as well as CNN benchmarks without data augmentation when the training set is small. For 100/200/500 training samples, the recognition accuracy of the MNIST dataset [16] is increased, respectively, from the figures of 68.33%/86.96%/91.33% reported by the CNNs optimized over architectures and dimensions [9] to, respectively, 81.55%/89.23%/93.11%. Similar improvements are also obtained in the EMNIST Letters dataset [4] and the Transformed MNIST datasets. The computational results reported here are for small datasets, which can be handled efficiently by LIBSVM [3].

## A. Background

In the early 2000s, SVMs [5] were one of the most popular and effective methods for image classification [18]. They also had a firm theoretical foundation [26], [1] of margin maximization that is especially important in high dimensions, a kernel

method to make high-dimensional computation tractable, and a loose upper bound on the expected generalization performance as the expected proportion of samples that are support vectors. Importantly, SVMs employed a reliable computational scheme based on quadratic programming.

However, with the advent of CNNs and the enhancement of computing power through graphics processing units (GPUs), SVMs were gradually replaced in image classification. One of the reasons for the success of CNNs was that they were able to incorporate prior knowledge into the neural network. Indeed, the pioneering paper of CNNs [29] makes the point that “It is usually accepted that good generalization performance on real-world problems cannot be achieved unless some a priori knowledge about the task is built into the system. Back-propagation networks provide a way of specifying such knowledge by imposing constraints both on the architecture of the network and on its weights. In general, such constraints can be considered as particular transformations of the parameter space.” It further mentions specifically that, “Multilayer constrained networks perform very well on this task when organized in a hierarchical structure with shift-invariant feature detectors.” Indeed, CNNs have successfully incorporated several important characteristics of images. One, mentioned above (called shift-invariance), is translational invariance, which is exploited by the constancy, i.e., location independence, of the convolution matrices. A second is locality. For example, an “edge” in an image can be recognized from just the neighboring pixels. This is exploited by the low dimensionality of the kernel matrix. A third characteristic is the multiplicity of spatial scales, i.e., a hierarchy of spatial “features” of multiple sizes in images. These three properties are captured in modern CNNs through the “pooling” operation at the  $(\ell+1)$ -th layer, where the features of the  $\ell$ -th layer are effectively low-pass filtered through operations such as max-pooling. More recently, it has been shown that depth in neural networks (NNs) of rectified linear units (ReLUs) permits composition, and enhances expressivity for a given number of parameters, as well as reducing the number of parameters needed for approximations of given accuracy [7].

With the wide availability of datasets such as CIFAR-10 [14] and ImageNet [8] for testing, there has been continued success in the empirical engineering of several high-performance CNN architectures, such as AlexNet [15], VGG16 [23], GoogLeNet [24], and ResNet [12], [13]. Generally, neural networks have tended to become larger over time with the number of parameters ranging into hundreds of millions. Concomitantly they have also become increasingly data-hungry. Such data-hungry NNs may be inappropriate for several applications where data is expensive or scarce, e.g., medical data [2]. For these reasons, there is an interest in methodologies for learning efficiently from very few samples, which is the focus of this paper.

## B. Related Work

There are mainly two studies related to our work: global invariant kernels and local correlations.

*a) Global Invariant Kernels:* To guarantee global invariance over all transformations, Haasdonk et al. [10], [11] proposed two invariant kernels. One, which they call “invariant integration,” takes an average over a transformation group. Although this kernel is trivially positive definite, it appears to produce poor results in our testing, as we will see in Section IV. Recently, Mei et al. [19] considered this in the context of kernel ridge regression (KRR) in the reproducing kernel Hilbert space (RKHS). Another kernel considered by [10] consists of transformations such as adding a constant value to the brightness values of all pixels, which is not relevant to the subject of this paper.

*b) Local Correlations:* Since “local correlations,” i.e., dependencies between nearby pixels, are more pronounced than long-range correlations in natural images, Scholkopf et al. [20] defined a two-layer kernel utilizing dot product in a polynomial space which is mainly spanned by local correlations between pixels. We extend the structure of such a two-layer local correlation to multilayer architectures by introducing further compositions, which gives the flexibility to consider the locality at multiple spatial scales. We also analyze the corresponding time and space complexity of multilayer architectures.

## II. KERNELS WITH TRANSFORMATIONAL INVARIANCE

To fix notation, let  $\mathcal{S} = \{(X_1, y_1), \dots, (X_n, y_n)\}$  be a set of labeled samples with  $X_i = (X_i^{(1)}, X_i^{(2)}, \dots, X_i^{(m)})^T \in \mathcal{X} \subset \mathbb{R}^m$  and  $y_i \in \mathcal{Y}$ . Here,  $\mathcal{X}$  and  $\mathcal{Y}$  represent the sample and label spaces respectively, with the number of samples  $n$  and the number of features  $m$ . We desire to fit a mapping  $h$  from  $\mathcal{X}$  to  $\mathcal{Y}$ .

### A. Transformation Groups and Transformation-Invariant Best-Fit Kernels

We wish to endow the kernel of the SVM with the domain knowledge that the sample classification is invariant under certain transformations of the sample vector. Let  $\mathcal{G}$  be a transformation group that acts on  $\mathcal{X}$ , i.e., for all  $S, T, U \in \mathcal{G}$ : (i)  $T$  maps  $\mathcal{X}$  into  $\mathcal{X}$ ; (ii) the identity map  $I \in \mathcal{G}$ ; (iii)  $ST \in \mathcal{G}$ ; (iv)  $(ST)U = S(TU)$ ; (v) there is an inverse  $T^{-1} \in \mathcal{G}$  with  $TT^{-1} = T^{-1}T = I$ .

We start with a base kernel  $K_{base} : \mathcal{X} \times \mathcal{X} \rightarrow \mathcal{R}$  that satisfies the following properties:

- 1) symmetric, i.e.,  $K_{base}(X_i, X_j) = K_{base}(X_j, X_i)$ ,
- 2) positive definite if its Gram matrix is positive semi-definite, i.e.,  $\sum_{i=1}^n \sum_{j=1}^n \alpha_i \alpha_j K_{base}(X_i, X_j) \geq 0$  for all  $\alpha_1, \dots, \alpha_n \in \mathbb{R}$ , and
- 3) which satisfies

$$K_{base}(TX_i, X_j) = K_{base}(X_i, T^{-1}X_j), \quad \forall T \in \mathcal{G}.$$

Define the kernel with the “best-fit” transformation over  $\mathcal{G}$  by

$$K_{\mathcal{G},best,base}(X_i, X_j) := \sup_{T \in \mathcal{G}} K_{base}(TX_i, X_j).$$

**Lemma 1.**  $K_{\mathcal{G},best,base}$  is a symmetric kernel that is also transformation-invariant over the group  $\mathcal{G}$ , i.e.,  $\forall T \in \mathcal{G}$ ,

$$K_{\mathcal{G},best,base}(TX_i, X_j) = K_{\mathcal{G},best,base}(X_i, X_j).$$

*Proof.* The symmetry follows since

$$\begin{aligned}
K_{\mathcal{G},\text{best},\text{base}}(X_i, X_j) &= \sup_{T \in \mathcal{G}} K_{\text{base}}(TX_i, X_j) \\
&= \sup_{T \in \mathcal{G}} K_{\text{base}}(X_i, T^{-1}X_j) = \sup_{T \in \mathcal{G}} K_{\text{base}}(T^{-1}X_j, X_i) \\
&= \sup_{T^{-1} \in \mathcal{G}} K_{\text{base}}(T^{-1}X_j, X_i) = K_{\mathcal{G},\text{best},\text{base}}(X_j, X_i).
\end{aligned}$$

The transformational invariance follows since

$$\begin{aligned}
K_{\mathcal{G},\text{best},\text{base}}(TX_i, X_j) &= \sup_{S \in \mathcal{G}} K_{\text{base}}(STX_i, X_j) \\
&= \sup_{UT^{-1} \in \mathcal{G}} K_{\text{base}}(UX_i, X_j) = \sup_{U \in \mathcal{G}} K_{\text{base}}(UX_i, X_j) \\
&= K_{\mathcal{G},\text{best},\text{base}}(X_i, X_j).
\end{aligned}$$

□

**The Translation Group:** Of particular interest in image classification is the group of translations. Let  $X_i = \{X_i^{(p,q)} : p \in [m_1], q \in [m_2]\}$  denote a two-dimensional  $m_1 \times m_2$  array of pixels, with  $m = m_1 m_2$ . Let  $T_{rs}X_i := \{X_i^{((p+r) \bmod m_1, (q+s) \bmod m_2)} : p \in [m_1], q \in [m_2]\}$  denote the transformation that translates the array by  $r$  pixels in the x-direction, and by  $s$  pixels in the y-direction. The translation group is  $\mathcal{G}_{\text{trans}} := \{T_{rs} : r \in [m_1], s \in [m_2]\}$ . For notational simplicity, we will denote the resulting kernel  $K_{\mathcal{G}_{\text{trans}},\text{best},\text{base}}$  by  $K_{\text{TI},\text{best},\text{base}}$ .

### B. Positive Definiteness of Translation-Invariant Best-Fit Kernels

There are two criteria that need to be met when trying to embed transformational invariance into SVM kernels. (i) The kernel will need to be invariant with respect to the particular transformations of interest in the application domain. (ii) The kernel will need to be positive definite to have provable guarantees of performance.

$K_{\text{TI},\text{best},\text{base}}$  satisfies property (i) as established in Lemma 1. Concerning property (ii) though, in general,  $K_{\text{TI},\text{best},\text{base}}$  is an indefinite kernel. We now show that when the base kernel is a normalized linear kernel,  $K_{\text{linear}}(X_i, X_j) := \frac{1}{m} X_i^T X_j$ , then it is indeed positive definite in the small sample regime of interest. Subsequently, in Theorem 2, we show that this also holds for polynomial kernels that are of importance in practice.

To prove positive definiteness, we need to assume a probabilistic model for dependent features.

**Assumption 1.** Suppose that the  $n$  samples  $\{X_1, X_2, \dots, X_m\}$  are i.i.d., with  $X_i = \{X_i^{(1)}, X_i^{(2)}, \dots, X_i^{(m)}\}$  being a normal random vector with  $X_i \sim \mathcal{N}(0, \Sigma)$ ,  $\forall i \in [n]$ . Suppose also that  $\|\lambda\|_2 / \|\lambda\|_\infty \geq (\ln m)^{\frac{1+\epsilon}{2}} / 2$  for some  $\epsilon \in (0, 1]$ , where  $\lambda := (\lambda^{(1)}, \dots, \lambda^{(m)})$  is comprised of the eigenvalues of  $\Sigma$ . Note that  $X_i$  and  $X_j$ ,  $j \neq i$  are independent, but  $X_i^{(p)}$  may be correlated with  $X_i^{(q)}$ , for  $p \neq q$ .

**Example 1.** When  $\Sigma = I_m$ , i.e.,  $X_i^{(p)} \sim \mathcal{N}(0, 1)$ ,  $\forall p \in [m]$ , the condition  $\|\lambda\|_2 / \|\lambda\|_\infty \geq (\ln m)^{\frac{1+\epsilon}{2}} / 2$  holds trivially since  $\|\lambda\|_2 = \sqrt{m}$  and  $\|\lambda\|_\infty = 1$ .

**Theorem 1.** Let

$$K_{\text{TI},\text{best},\text{linear}}(X_i, X_j) := \sup_{T \in \mathcal{G}_{\text{trans}}} \frac{1}{m} (TX_i)^T X_j$$

be the best-fit translation invariant kernel with the base kernel chosen as the normalized linear kernel. Under Assumption 1, if  $n \leq \frac{\|\lambda\|_1}{2\|\lambda\|_2(\ln m)^{\frac{1+\epsilon}{2}}}$ , then  $K_{\text{TI},\text{best},\text{linear}}$  is a positive definite kernel with probability approaching one, as  $m \rightarrow \infty$ .

*Outline of proof.* We briefly explain the ideas behind the proof of Theorem 1, with details presented in the Appendix B. For brevity, we denote  $K_{\text{TI},\text{best},\text{linear}}(X_i, X_j)$  and  $K_{\text{linear}}(X_i, X_j)$  by  $K_{\text{TI},ij}$  and  $K_{ij}$ , respectively. From Gershgorin's circle theorem [27] every eigenvalue of  $K_{\text{TI},\text{best},\text{linear}}$  lies within at least one of the Gershgorin discs  $\mathcal{D}(K_{\text{TI},ii}, r_i) := \{\lambda \in \mathbb{R} \mid |\lambda - K_{\text{TI},ii}| \leq r_i\}$ , where  $r_i := \sum_{j \neq i} |K_{\text{TI},ij}|$ . Hence if  $K_{\text{TI},ii} > \sum_{j \neq i} |K_{\text{TI},ij}|$ ,  $\forall i$ , then  $K_{\text{TI}}$  is a positive definite kernel. Accordingly, we study a tail bound on  $\sum_{j \neq i} |K_{\text{TI},ij}|$  and an upper bound on  $K_{\text{TI},ii}$ , respectively, to finish the proof. □

Note that  $\|\lambda\|_1 \leq \sqrt{m}\|\lambda\|_2$  for  $m$ -length vector  $\lambda$ , which implies that  $n = \tilde{O}(\sqrt{m})$ .

We now show that the positive definiteness in the small sample regime also holds for the polynomial kernels which are of importance in practice:

$$K_{\text{poly}}(X_i, X_j) := (1 + \gamma X_i^T X_j)^d \text{ for } \gamma \geq 0 \text{ and } d \in \mathbb{N}.$$

**Theorem 2.** For any  $\gamma \in \mathbb{R}_+$  and  $d \in \mathbb{N}$ , the translation-invariant kernels,

$$K_{\text{TI},\text{best},\text{poly}}(X_i, X_j) := \sup_{T \in \mathcal{G}_{\text{trans}}} (1 + \gamma (TX_i)^T X_j)^d$$

are positive definite with probability approaching 1 as  $m \rightarrow +\infty$ , under Assumption 1 and  $n \leq \frac{\|\lambda\|_1}{2\|\lambda\|_2(\ln m)^{\frac{1+\epsilon}{2}}}$ .

*Proof.* Due to monotonicity,

$$\begin{aligned}
K_{\text{TI},\text{best},\text{poly}}(X_i, X_j) &:= \sup_{T \in \mathcal{G}_{\text{trans}}} (1 + \gamma (TX_i)^T X_j)^d \\
&= (1 + \gamma \sup_{T \in \mathcal{G}_{\text{trans}}} (TX_i)^T X_j)^d \\
&= (1 + \gamma m K_{\text{TI},\text{best},\text{linear}}(X_i, X_j))^d.
\end{aligned}$$

Now note that if  $K_1$  and  $K_2$  are positive definite kernels, then the following kernels  $K$  obtained by Schur products [21], addition, or adding a positive constant elementwise, are still positive definite kernels:

$$\begin{aligned}
K_{ij} &= \alpha K_{1,ij} + \beta K_{2,ij}, \forall \alpha, \beta \geq 0, \\
K_{ij} &= (K_{1,ij})^{\ell_1} (K_{2,ij})^{\ell_2}, \forall \ell_1, \ell_2 \in \mathbb{N}, \\
K_{ij} &= K_{1,ij} + \gamma, \forall \gamma \geq 0.
\end{aligned} \tag{1}$$

Since  $K_{\text{TI},\text{best},\text{poly}}$  can indeed be obtained by repeatedly applying the above operations starting with  $K_{\text{TI},\text{best},\text{linear}}$ , it follows that  $K_{\text{TI},\text{best},\text{poly}}$  is positive definite whenever  $K_{\text{TI},\text{best},\text{linear}}$  is, which holds with probability approaching one as  $m \rightarrow +\infty$ . □

TABLE I

THE VALUE OF  $n$  UP TO WHICH THE KERNEL IS POSITIVE DEFINITE. THIS SEEMS TO INDICATE THAT POSITIVE DEFINITENESS CONTINUES TO HOLD FOR MODERATE SAMPLE SIZES, AND THAT THE THEOREM PROVIDED IS CONSERVATIVE.

Datasets	$K_{TI,best,linear}$	$K_{TI,best,poly}$
Original MNIST	$\approx 45$	$\approx 375$
EMNIST	$\approx 35$	$\approx 395$
Translated MNIST	$\approx 455$	$\approx 15000$

**Remark.** Since Gershgorin's circle theorem is a conservative bound for the eigenvalues of a matrix, the bound of  $n = \tilde{O}(\sqrt{m})$  on the number of samples is also a conservative condition for positive definiteness. In practice, larger  $n$  also yields positive definiteness of  $K_{TI,best,linear}$ . Even more usefully,  $K_{TI,best,poly}$  is positive definite for a much larger range of  $n$  than  $K_{TI,best,linear}$ , as reported in Table I.

### C. Comparison with the Average-Fit Kernel and Data Augmentation

1) *Average-Fit Kernel:* In [10], the “average-fit kernel”

$$K_{\mathcal{G}_{trans},avg,linear}(X_i, X_j) := \frac{1}{|\mathcal{G}|} \sum_{T \in \mathcal{G}} K_{linear}(TX_i, X_j) \quad (2)$$

is considered, which seeks the “average” fit over all transformations. Such a kernel is trivially invariant with respect to the transformations in  $\mathcal{G}$  and positive definite. However, it is not really a desirable choice for the case of translations when the base kernel is the linear kernel, since the average-fit kernel  $K_{\mathcal{G}_{trans},avg,linear}(X_i, X_j)$ , denoted by  $K_{TI,avg,linear}(X_i, X_j)$  for short, satisfies

$$K_{TI,avg,linear}(X_i, X_j) = \left( \frac{1}{|\mathcal{G}_{trans}|} \sum_{T \in \mathcal{G}_{trans}} TX_i \right)^T X_j.$$

Note that  $\frac{1}{|\mathcal{G}_{trans}|} \sum_{T \in \mathcal{G}_{trans}} TX_i = \alpha(1, 1, \dots, 1)^T$ , where  $\alpha = \frac{1}{m} \sum_{p \in [m_1], q \in [m_2]} X_i^{(p,q)}$  is the average brightness level of  $X_i$ . Therefore  $K_{TI,avg,linear}(X_i, X_j) = m \times (\text{Avg brightness level of } X_i) \times (\text{Avg brightness level of } X_j)$ . The kernel solely depends on the average brightness levels of the samples, which basically blurs out all detail in the samples. In the case of rotational invariance, it will only depend on the average brightness along each concentric circle's circumference. As expected, the SVM employing this average-fit kernel produces very poor results, as we will see in the experimental results reported in Section IV.

2) *Data Augmentation:* Data augmentation is a popular approach to learn how to recognize translated images. This approach augments the dataset by creating several translated copies of the existing samples. When applying SVM with kernel  $K_{base}$  to the augmented data, it is equivalent to employing the average-fit kernel as (2). This can be seen as follows. Consider the case where the augmented data consists of all translates of

each image. Then the resulting dual problem for SVM margin maximization [5] is:

$$\begin{aligned} \max_{\lambda} & -\frac{1}{2} \sum_{i,j,T_1,T_2} \lambda_{i,T_1} \lambda_{j,T_2} y_i y_j K(T_1 X_i, T_2 X_j) + \sum_{i,T} \lambda_{i,T} \\ \text{s.t. } & \lambda_{i,T} \geq 0, \forall i \in [n], \forall T \in \mathcal{G}_{trans}; \sum_{i,T} \lambda_{i,T} y_i = 0, \end{aligned}$$

where  $K$  represents  $K_{base}$  above. The corresponding classifier is  $\text{sign}(\sum_{i,T} \lambda_{i,T}^* y_i K_{base}(TX_i, X) + b^*)$ , where  $\lambda^*$ 's are the optimal dual variables and  $b^* = y_j - \sum_{i,T} \lambda_{i,T}^* y_i K_{base}(TX_i, T'X_j)$ , for any  $j$  and  $T'$  satisfying  $\lambda_{j,T'}^* > 0$ . When no data augmentation is implemented, i.e.,  $|\mathcal{G}_{trans}| = 1$ , we will use  $\lambda_i$  as shorthand for  $\lambda_{i,1}$ . As shown in Theorem 4.1 of [17], this is simply the dual problem for the SVM with  $K_{TI,avg,base}$ , and  $\forall j$ ,

$$\sum_i \lambda_i K_{TI,avg,base}(X_i, X_j) = \sum_{i,T \in \mathcal{G}} \lambda_{i,T} K_{base}(TX_i, X_j).$$

Hence data augmentation is mathematically equivalent to a kernel with the average similarity over all transformations. As we have seen above, this yields a poor classifier since it only leverages the average brightness level of an image.

We give a simple example to illustrate the superiority of  $K_{TI,best,linear}$  over  $K_{TI,avg,linear}$  or data augmentation.

*Example 1.* Consider a training set with just two samples  $X_1 = (1, 2)$  and  $X_2 = (5, 2)$ , shown in red in Figure 1. Two new samples  $X_3 = (2, 1)$  and  $X_4 = (2, 5)$  are generated through data augmentation, shown in green. The decision boundary of the based kernel with augmented data (equivalent to the average-fit kernel  $K_{TI,avg}$ ) is shown by the blue solid line in Figure 1. Note that the decision boundary  $X^{(1)} + X^{(2)} = 5$  depends solely on the brightness level  $X^{(1)} + X^{(2)}$ .

However, the decision boundary of the best-fit kernel  $K_{TI,best,linear}(X_i, X_j) = \sup_{T \in \mathcal{G}_{trans}} \frac{1}{2} (TX_i)^T X_j$  is piecewise linear due to the “sup” operation. Since each piece focuses on half of the samples that are on the same side of the symmetry axis (red dashed line), it leads to a larger margin, as shown by the orange piece-wise linear separatrix. For other kernels (e.g., polynomial kernels), the shape of the decision boundary will be altered correspondingly (e.g., piecewise polynomial), but the TI best-fit kernel can still maintain a larger margin.

### D. Rotation-Invariant Kernels

To mathematically treat the case of rotation-invariant kernels, we consider images that are circular, of radius  $r$ , with each concentric annulus from radius  $\frac{(p-1)r}{m_1}$  to  $\frac{pr}{m_1}$ , for  $p \in [m_1]$ , comprised of  $m_2$  pixels spanning the sectors  $[2k\pi/m_2, 2(k+1)\pi/m_2]$  for  $k = 0, 1, \dots, m_2 - 1$ . Denote the element in the  $p$ -th annulus and  $q$ -th sector as “pixel”  $X^{(p,q)}$ , and define the rotation group  $\mathcal{G}_{rotate} := \{T_1, T_2, \dots, T_{m_2}\}$ , where  $T_{q'} X^{(p,q)} = X^{(p,q+q')}$ . Correspondingly, we can define the rotation-invariant (RI) best-fit kernel as<sup>1</sup>

$$K_{RI,best,base}(X_i, X_j) := \sup_{T \in \mathcal{G}_{rotate}} K_{base}(TX_i, X_j).$$

<sup>1</sup>For notational simplicity, we will denote the resulting kernel  $K_{\mathcal{G}_{rotate},best,base}$  by  $K_{RI,best,base}$ .

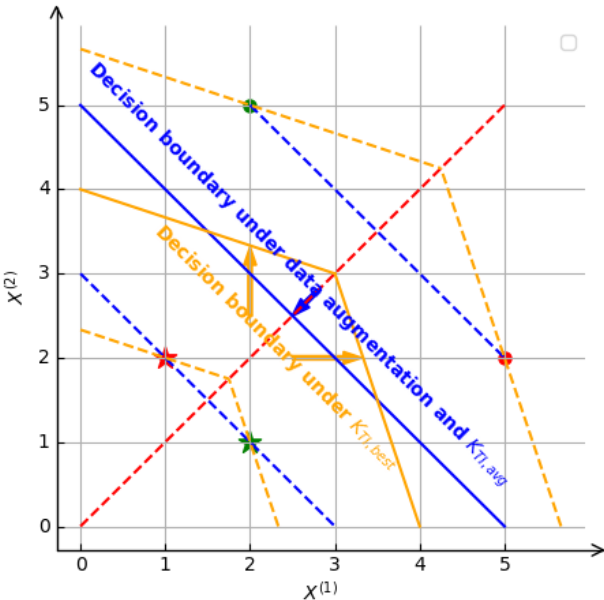


Fig. 1. The kernel  $K_{TI,best,linear}$  produces the piecewise linear separatrix shown in orange. It yields a larger margin than the blue separatrix that data augmentation and  $K_{TI,avg}$  yields.

A similar proof as for the RI best-fit kernel yields:

**Lemma 2.** *Under Assumption 1, the rotational invariant kernels  $K_{RI,best,poly}$  is positive definite with probability approaching one as  $m \rightarrow +\infty$ , under the same conditions as in Theorem 1.*

In practice, we place the original image in the middle of a larger canvas and rotate it. In this way, the information of the original object is preserved, and the blank area after rotation is filled with Gaussian noise. In Section IV, we report the large performance gain obtained by using an SVM with kernel  $K_{RI,best,poly}$ .

### III. INCORPORATING LOCALITY AT MULTIPLE SPATIAL SCALES

To better illustrate the property of “locality” and its incorporation into SVMs, we consider the simple context of a polynomial kernel and a one-dimensional real-valued pixel sequence.

Let us regard the individual pixel values in the sequence  $\{X_i^{(1)}, X_i^{(2)}, \dots, X_i^{(m)}\}$  as the primitive features at “Layer 0”. Consider now a “local” feature only depends on the nearby pixels  $\{X_i^{(\ell)}, X_i^{(\ell+1)}, \dots, X_i^{(\ell+k_1)}\}$  that can be modeled by a polynomial of degree  $d_1$ . We refer to  $k_1$  as the locality parameter.

Such a local feature is a linear combination of monomials of the form  $\prod_{j=\ell}^{\min(\ell+k_1, m)} (X_i^{(j)})^{c_j}$  with  $\sum_{j=\ell}^{\min(\ell+k_1, m)} c_j \leq d_1$  where each integer  $c_j \geq 0$ . This gives rise to a kernel

$$K_{L,ij}^{(1)} := \left[ \sum_{\ell=1}^{m-k_1} \left( \sum_{p=\ell}^{\ell+k_1} X_i^{(p)} X_j^{(p)} + 1 \right)^{d_1} + 1 \right]^{d_2}. \quad (3)$$

We regard “Layer 1” as comprised of such local features of locality parameter  $k_1$ , i.e., at most  $k_1$  apart.

“Layer 2” allows the composition of local features at Layer 1 that are at most  $k_2$  apart:

$$K_{L,ij}^{(2)} := \left\{ \sum_{g=1}^{m-k_1-k_2} \left[ \sum_{\ell=g}^{g+k_2} \left( \sum_{p=\ell}^{\ell+k_1} X_i^{(p)} X_j^{(p)} + 1 \right)^{d_1} \right]^{d_2} + 1 \right\}^{d_3}.$$

This can be recursively applied to define deeper kernels with locality at several coarser spatial scales.

The above procedure extends naturally to two-dimensional images  $\{X_i^{(p,q)} : p \in [m_1], q \in [m_2]\}$ . Then the kernel at Layer 1 is simply  $(\sum_{s=1}^{m_2-k_1} \sum_{\ell=1}^{m_1-k_1} (\sum_{q=s}^{s+k_2} \sum_{p=\ell}^{\ell+k_1} X_i^{(p,q)} X_j^{(p,q)} + 1)^{d_1} + 1)^{d_2}$ . The resulting kernels are always positive definite:

**Lemma 3.**  *$K_L$  is a positive definite kernel.*

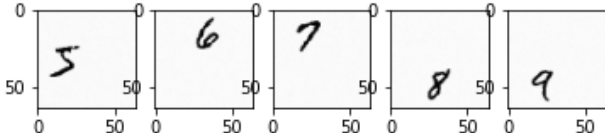
*Proof.* The result follows from the properties of positive definite kernels in Theorem 2, since the kernel  $K_L$  can be obtained by repeatedly employing the operations in (1) with  $\alpha = \beta = \gamma = 1$ , starting with a base linear kernel.  $\square$

One difference from CNNs is that, for the same input layer, one cannot have multiple output channels. The reason is that if we design multiple channels with different degrees, then the channel with a larger degree will automatically subsume all terms generated by the channel with a smaller degree. Therefore, it is equivalent to having only one output channel with the largest degree. On the other hand, if the images have multiple channels to start with (as in R, G, and B, for example), then they can be handled separately. But after they are combined at a layer, there can only be one channel at subsequent higher layers.

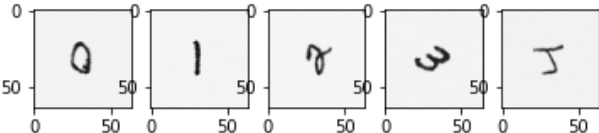
a) *Combining Locality at Multiple Spatial Scales with Transformational Invariance:* To combine both locality at multiple spatial scales and transformational invariance, a kernel with locality at multiple spatial scales can be introduced as a base kernel into transformation-invariant kernels.

b) *Complexity Analysis and Memory Trade-off:* One may trade off between the memory requirement and computation time when it comes to the depth of the architecture. Supported by adequate memory space, one can store all kernel values from every layer, with both computation time and memory space increasing linearly with depth. In contrast, when limited by memory space, one can store only the kernel values from the final layer. In that case, although the memory requirement does not increase with depth, computation time grows exponentially with depth.

The time complexity of computing the polynomial kernel is between  $O(n^2m)$  and  $O(n^3m)$  based on LIBSVM [3], while space complexity is  $O(n^2)$ . With sufficient memory of order  $O(n^2m)$ , the computations of kernel values can be parallelized so that the time complexity of the locality kernel is considerably



(a) Translated MNIST (T-MNIST).



(b) Rotated MNIST (R-MNIST).

Fig. 2. Transformed MNIST with random translation/rotation and Gaussian noise ( $\mu = 0, \sigma = 0.1$ ).

reduced to between  $O(n^2kd)$  and  $O(n^3kd)$ , where  $k$  and  $d$  are the locality parameter and the depth, respectively, with  $kd \ll m$ .

#### IV. EXPERIMENTAL EVALUATION

##### A. Datasets

We evaluate the performance of the methods developed on four datasets:

- 1) The Original MNIST Dataset [16]
- 2) The EMNIST Letters Dataset [4]
- 3) The Translated MNIST Dataset: Since most generally available datasets appear to have already been centered or otherwise preprocessed, we “uncenter” them to better verify the accuracy improvement of TI kernels. We place the objects in a larger (64\*64\*1) canvas, and then randomly translate them so that they are not necessarily centered but still maintain their integrity. In addition, we add a Gaussian noise ( $\mu = 0, \sigma = 0.1$ ) to avoid being able to accurately center the image by calculating the center-of-mass. We call the resulting dataset the “Translated dataset”. Figure 2a shows some samples from different classes of the Translated MNIST dataset.
- 4) The Rotated MNIST Dataset: Similarly, we also create a “Rotated dataset”. (We skip the digits “6” and “9” since they are equivalent after 180° rotation.) Figure 2b displays some samples from different classes of the Rotated MNIST dataset.

##### B. Experimental Results and Observations

Table II and Figure 3 provide the test accuracy of all methods on the Original and Transformed MNIST Datasets, respectively, while Table III shows the test accuracy for the EMNIST Letters Dataset [4]. In the Tables and Figure 3, the letters L, TI, RI represent Locality at multiple spatial scales, TI kernels, and RI kernels, respectively. A combination such as L-TI represents an SVM that uses both Locality as well as Translational Invariance.

For the Original MNIST dataset with 100/200/500 training samples (Table II), after introducing locality and transformational invariance, the classification accuracy is improved from 68.33%/86.96%/91.33% reported by the best

TABLE II  
ORIGINAL MNIST DATASET (100, 200, 500 TRAINING SAMPLES): TEST ACCURACY OF NEWLY PROPOSED METHODS COMPARED WITH THE ORIGINAL SVM, THE RI-SVM BASED ON AVERAGE FIT, AND THE BEST CNN.

Method	100	200	500
	Acc/%	Acc/%	Acc/%
L-TI-RI-SVM	<b>81.55</b>	<b>89.23</b>	92.58
TI-RI-SVM	75.10	86.47	<b>93.11</b>
L-TI-SVM	78.86	87.02	91.01
L-RI-SVM	77.96	83.96	89.65
TI-SVM	69.34	82.34	91.00
RI-SVM	73.82	83.60	90.19
L-SVM	75.27	82.11	88.21
SVM	68.16	78.67	87.14
RI-SVM (Average-Fit)	68.05	78.81	87.21
Best CNN <sup>3</sup>	68.33	86.96	91.33

CNNs optimized over architectures and dimensions [9] to 81.55%/89.23%/93.11% respectively. The small but tangible improvements indicate that the original dataset does not center and deskew objects perfectly. Larger improvements can be observed on the EMNIST Letters dataset [4] in Table III compared with the original SVM, RI kernel based on Average-Fit and ResNet. Note that all test accuracies displayed in the tables are multi-class classification accuracies <sup>2</sup>.

In Figure 3, we present the obtained test accuracies as a function of the number of training samples, for two different transformed datasets. Experiments are performed 10 times with mean and standard deviation denoted by the length of the bars around the mean, for 100/300/500/700/1000 training samples respectively. (L-)TI-SVM and (L-)RI-SVM outperform ResNet in many cases when there is no data augmentation since they embed useful domain knowledge for classifiers, especially for the small size regime of training samples. However, with the increase in the number of training samples, the benefits brought by domain knowledge gradually decrease, as shown in Figure 3. Additionally, the test accuracies of the newly proposed methods have a smaller variance than ResNet’s in general.

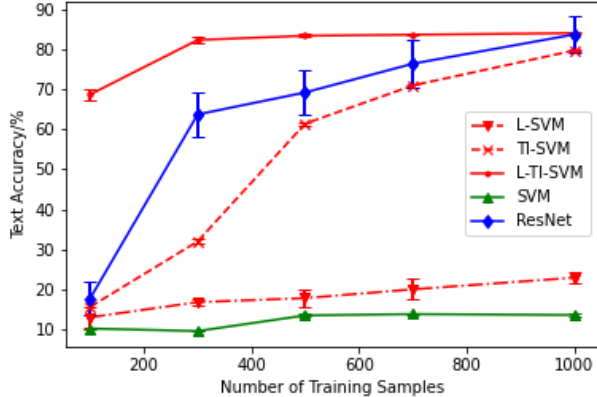
From the experimental results, we see that all SVMs with newly defined kernels improve upon the test accuracy of the original SVM method, whether they are original datasets or transformed datasets. They also greatly outperform the best CNNs in the small training sample regime of interest. For transformed datasets, improvements are more significant.

##### C. Details of Experimental Evaluation

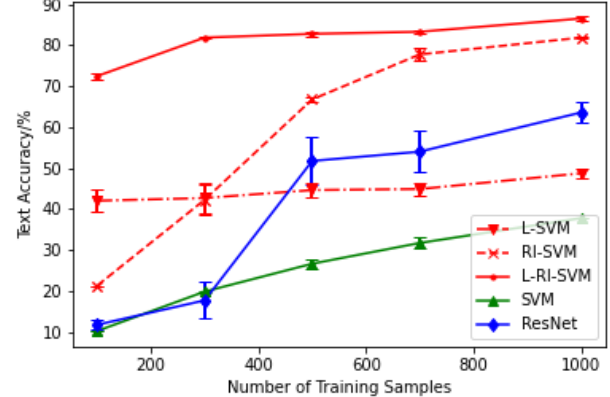
With consideration of computational speed and memory space, we utilize a two-layer structure (3) as well as a  $\frac{k_1-1}{2}$ -zero padding and a stride of 1 to implement locality. In order to compare the test accuracy of L-SVM, TI-SVM, RI-SVM

<sup>2</sup>One may also note that multi-class classification is actually not even an inherent forte of SVMs, since it is accomplished through several binary classifications, further indicating the effectiveness of the newly developed methods.

<sup>3</sup>Since [9] did not provide test accuracy for 200 training samples, we use a fine-tuned ResNet to fill in the gaps.



(a) Translated MNIST.



(b) Rotated MNIST.

Fig. 3. Test accuracy vs. Number of training samples, for Transformed MNIST datasets. L-TI-SVM yields considerable improvement at small sizes in the case of translated samples, while, similarly, L-RI-SVM does so in the case of rotated samples.

TABLE III  
EMNIST LETTERS DATASET (100, 200, 500 TRAINING SAMPLES): TEST ACCURACY OF NEWLY PROPOSED METHODS COMPARED WITH THE ORIGINAL SVM, RI-SVM BASED ON AVERAGE-FIT, AND RESNET.

Method	100	200	500
	Acc/%	Acc/%	Acc/%
L-TI-RI-SVM	<b>44.56</b>	<b>55.18</b>	66.42
TI-RI-SVM	43.16	52.40	<b>67.42</b>
L-TI-SVM	42.51	52.81	64.66
L-RI-SVM	38.39	47.29	59.76
TI-SVM	39.94	48.12	63.52
RI-SVM	38.03	45.02	59.04
L-SVM	37.01	45.08	58.05
SVM	36.65	42.74	56.38
RI-SVM (Average-Fit)	36.82	42.41	56.22
ResNet	11.48	41.17	61.12

and further combine them, we select a polynomial kernel with a fixed degree (8 in our experiments) to realize the proposed methods. Note that degree 8 is not necessarily the optimal degree; one can tune the specific degree for different datasets.

We compare our results with [9], which adopts a tree building technique to examine all the possible combinations of layers and corresponding dimensionalities to find the optimal CNN architecture. As for the DNN benchmark of the EMNIST Letters and the Transformed MNIST datasets, we select ResNet [12], [13], a classic CNN architecture, as a DNN benchmark. Plus, for fairness, we do not implement data augmentation for ResNet and train all models from scratch.

Note that all experimental results are based on LIBSVM [3] and are carried out on an Intel Xeon E5-2697A V4 Linux server with a maximum clock rate of 2.6 GHz and a total memory of 512 GB.

## V. CONCLUDING REMARKS

In this paper, we have developed transformation-invariant kernels that capture domain knowledge of the invariances in the

domain. They can also additionally incorporate composition and locality at multiple spatial scales. The resulting kernels appear to provide significantly superior classification performance in the small sample size regime that is of interest in this paper. Experiments demonstrate that for the same polynomial kernel, incorporating locality and transformational invariance improves accuracy, especially for situations where data is scarce. This work can be applied to fields other than image classification if such domain knowledge holds.

## ACKNOWLEDGEMENT

This material is based upon work partially supported by US National Science Foundation under CMMI-2038625, HDR Tripods CCF-1934904; US Office of Naval Research under N00014-21-1-2385; US ARO under W911NF2120064, W911NF1810331; and U.S. Department of Energy's Office of Energy Efficiency and Renewable Energy (EERE) under the Solar Energy Technologies Office Award Number DE-EE0009031. The views expressed herein and conclusions contained in this document are those of the authors and should not be interpreted as representing the views or official policies, either expressed or implied, of the U.S. NSF, ONR, ARO, Department of Energy or the United States Government. The U.S. Government is authorized to reproduce and distribute reprints for Government purposes notwithstanding any copyright notation herein.

## REFERENCES

- [1] B. E. Boser, I. M. Guyon, and V. N. Vapnik. A training algorithm for optimal margin classifiers. In *Proceedings of the Fifth Annual Workshop on Computational Learning Theory*, pages 144–152, 1992.
- [2] D. C. Castro, I. Walker, and B. Glocker. Causality matters in medical imaging. *Nature Communications*, 11(1):1–10, 2020.
- [3] C.-C. Chang and C.-J. Lin. Libsvm: A library for support vector machines. *ACM transactions on intelligent systems and technology (TIST)*, 2(3):1–27, 2011.
- [4] G. Cohen, S. Afshar, J. Tapson, and A. Van Schaik. Emnist: Extending mnist to handwritten letters. In *2017 International Joint Conference on Neural Networks (IJCNN)*, pages 2921–2926. IEEE, 2017.

- [5] C. Cortes and V. Vapnik. Support-vector networks. *Machine learning*, 20(3):273–297, 1995.
- [6] E. D. Cubuk, B. Zoph, D. Mane, V. Vasudevan, and Q. V. Le. Autoaugment: Learning augmentation policies from data. *Conference on Computer Vision and Pattern Recognition*, 2019.
- [7] I. Daubechies, R. DeVore, S. Foucart, B. Hanin, and G. Petrova. Nonlinear approximation and (deep) relu networks. *Constructive Approximation*, pages 1–46, 2021.
- [8] J. Deng, W. Dong, R. Socher, L.-J. Li, K. Li, and L. Fei-Fei. Imagenet: A large-scale hierarchical image database. In *2009 IEEE conference on computer vision and pattern recognition*, pages 248–255. Ieee, 2009.
- [9] R. N. D’Souza, P.-Y. Huang, and F.-C. Yeh. Structural analysis and optimization of convolutional neural networks with a small sample size. *Scientific Reports*, 10(1):1–13, Nature Publishing Group, 2020.
- [10] B. Haasdonk and H. Burkhardt. Invariant kernel functions for pattern analysis and machine learning. *Machine learning*, 68(1):35–61, 2007.
- [11] B. Haasdonk and H. Burkhardt. Classification with invariant distance substitution kernels. In *Data Analysis, Machine Learning and Applications*, pages 37–44. Springer, 2008.
- [12] K. He, X. Zhang, S. Ren, and J. Sun. Deep residual learning for image recognition. In *Proceedings of the IEEE conference on computer vision and pattern recognition*, pages 770–778, 2016.
- [13] K. He, X. Zhang, S. Ren, and J. Sun. Identity mappings in deep residual networks. In *European conference on computer vision*, pages 630–645. Springer, 2016.
- [14] A. Krizhevsky, G. Hinton, et al. Learning multiple layers of features from tiny images. 2009.
- [15] A. Krizhevsky, I. Sutskever, and G. E. Hinton. Imagenet classification with deep convolutional neural networks. In *Advances in neural information processing systems*, pages 1097–1105, 2012.
- [16] Y. LeCun and C. Cortes. MNIST handwritten digit database. 2010.
- [17] Z. Li, R. Wang, D. Yu, S. S. Du, W. Hu, R. Salakhutdinov, and S. Arora. Enhanced convolutional neural tangent kernels. *arXiv preprint arXiv:1911.00809*, 2019.
- [18] D. Lu and Q. Weng. A survey of image classification methods and techniques for improving classification performance. *International journal of Remote sensing*, 28(5):823–870, 2007.
- [19] S. Mei, T. Misiakiewicz, and A. Montanari. Learning with invariances in random features and kernel models. *Conference on Learning Theory*, 2021.
- [20] B. Schölkopf, P. Simard, A. J. Smola, and V. Vapnik. Prior knowledge in support vector kernels. In *Advances in neural information processing systems*, pages 640–646, 1998.
- [21] J. Schur. Bemerkungen zur theorie der beschränkten bilinearformen mit unendlich vielen veränderlichen. 1911.
- [22] C. Shorten and T. M. Khoshgoftaar. A survey on image data augmentation for deep learning. *Journal of Big Data*, 6(1):1–48, 2019.
- [23] K. Simonyan and A. Zisserman. Very deep convolutional networks for large-scale image recognition. *International Conference on Learning Representations*, 2015.
- [24] C. Szegedy, W. Liu, Y. Jia, P. Sermanet, S. Reed, D. Anguelov, D. Erhan, V. Vanhoucke, and A. Rabinovich. Going deeper with convolutions. In *Proceedings of the IEEE conference on computer vision and pattern recognition*, pages 1–9, 2015.
- [25] M. Tan and Q. Le. Efficientnet: Rethinking model scaling for convolutional neural networks. In *International Conference on Machine Learning*, pages 6105–6114. PMLR, 2019.
- [26] V. N. Vapnik. *The nature of statistical learning theory*. Springer, 1995.
- [27] R. S. Varga. *Geršgorin and his circles*, volume 36. Springer Science & Business Media, 2010.
- [28] M. J. Wainwright. *High-dimensional statistics: A non-asymptotic viewpoint*, volume 48. Cambridge University Press, 2019.
- [29] Y. le Cun. Generalization and network design strategies. *Connectionism in perspective*, 19:143–155, 1989.

## APPENDIX

### A. Supporting Definitions and Lemmas

**Definition 1.** A random variable  $X$  with mean  $\mu = \mathbb{E}[X]$  is *sub-exponential* if there are non-negative parameters  $(\nu, b)$  such that [28]

$$\mathbb{E}[\exp(\lambda(X - \mu))] \leq \exp\left(\frac{\nu^2 \lambda^2}{2}\right), \quad \forall |\lambda| < \frac{1}{b}.$$

We denote this by  $X \sim SE(\nu, b)$ .

**Lemma 4** (Sub-exponential tail bound [28]). *Suppose that  $X \sim SE(\nu, b)$ . Then,*

$$\mathbb{P}[|X - \mu| \geq t] \leq \begin{cases} 2 \exp\left(-\frac{t^2}{2\nu^2}\right) & \text{if } 0 \leq t \leq \frac{\nu^2}{b}, \\ 2 \exp\left(-\frac{t}{2b}\right) & \text{if } t > \frac{\nu^2}{b}. \end{cases}$$

Some sub-exponential related properties are listed below.

**Lemma 5** ([28]). *a For standard normal random variable  $X$ ,  $X^2$  is  $SE(2, 4)$ ;*

*b For random variable  $X \sim SE(\nu, b)$ ,  $aX \sim SE(a\nu, ab)$ ;*

*c Consider independent random variables  $X_1, \dots, X_n$ , where  $X_i \sim SE(\nu_i, b_i)$ . Let  $\nu = (\nu_1, \dots, \nu_n)$  and  $b = (b_1, \dots, b_n)$ . Then  $\sum_{i=1}^n X_i \sim SE(\|\nu\|_2, \|b\|_\infty)$ .*

### B. Proof of Theorem 1

**Theorem 3** (Restatement of Theorem 1). *Let*

$$K_{TI,best,linear}(X_i, X_j) := \sup_{T \in \mathcal{G}_{trans}} \frac{1}{m} (TX_i)^T X_j$$

be the best-fit translation invariant kernel with the base kernel chosen as the normalized linear kernel. Under Assumption 1, if  $n \leq \frac{\|\lambda\|_1}{2\|\lambda\|_2(\ln m)^{\frac{1+\epsilon}{2}}}$ , then  $K_{TI,best,linear}$  is a positive definite kernel with probability approaching one, as  $m \rightarrow \infty$ .

*Proof of Theorem 1.* For brevity, we denote  $K_{TI,best,linear}(X_i, X_j)$  and  $K_{linear}(X_i, X_j)$  by  $K_{TI,ij}$  and  $K_{ij}$ , respectively. From Gershgorin's circle theorem [27] every eigenvalue of  $K_{TI,best,linear}$  lies within at least one of the Gershgorin discs  $\mathcal{D}(K_{TI,ii}, r_i) := \{\lambda \in \mathbb{R} \mid |\lambda - K_{TI,ii}| \leq r_i\}$ , where  $r_i := \sum_{j \neq i} |K_{TI,ij}|$ . Hence if  $K_{TI,ii} > \sum_{j \neq i} |K_{TI,ij}|$ ,  $\forall i$ , then  $K_{TI,best,linear}$  is a positive definite kernel.

Note that the dimension of the vector  $X_i$  is  $m = m_1 \times m_2$  in the case of a two-dimensional array. Under Assumption 1,  $X_i \sim \mathcal{N}(0, \Sigma)$ ,  $\forall i \in [n]$ . Since  $\Sigma$  is symmetric and positive semi-definite, there exists an orthogonal matrix  $O \in \mathbb{R}^{m \times m}$  with  $\Sigma = O \cdot \text{diag}(\lambda^{(1)}, \dots, \lambda^{(m)}) \cdot O^T$ , where  $\lambda^{(1)}, \dots, \lambda^{(m)} \geq 0$  are the eigenvalues of  $\Sigma$ . Define  $\Sigma^{\frac{1}{2}} := O \cdot \text{diag}(\sqrt{\lambda^{(1)}}, \dots, \sqrt{\lambda^{(m)}}) \cdot O^T$ , then  $X_i = \Sigma^{\frac{1}{2}} Z_i$ , where  $Z_i \sim \mathcal{N}(0, I_m)$ . Define  $H_i := O^T Z_i \sim \mathcal{N}(0, I_m)$ , then

$$\begin{aligned} \|X_i\|^2 &= \left\| O \text{diag}(\sqrt{\lambda^{(1)}}, \dots, \sqrt{\lambda^{(m)}}) O^T Z_i \right\|^2 \\ &= \left\| \text{diag}(\sqrt{\lambda^{(1)}}, \dots, \sqrt{\lambda^{(m)}}) H_i \right\|^2 = \sum_{p=1}^m \lambda^{(p)} (H_i^{(p)})^2, \end{aligned}$$

and  $\mathbb{E}[\|X_i\|^2] = \sum_{p=1}^m \lambda^{(p)} \mathbb{E}[(H_i^{(p)})^2] = \|\lambda\|_1$ .

Let  $\lambda := (\lambda^{(1)}, \dots, \lambda^{(m)})$ . Based on Lemma 5, we have  $(H_i^{(p)})^2 \sim SE(2, 4)$ ,  $\lambda^{(p)} (H_i^{(p)})^2 \sim SE(2\lambda^{(p)}, 4\lambda^{(p)})$ , and  $\|X_i\|^2 \sim SE(2\|\lambda\|_2, 4\|\lambda\|_\infty)$ . According to Lemma 4,

$$\mathbb{P}\left[\frac{1}{m} \|X_i\|^2 \leq \frac{\|\lambda\|_1}{m} - \frac{t}{m}\right] \leq \begin{cases} \exp\left(-\frac{t^2}{8\|\lambda\|_2^2}\right) & \text{if } 0 \leq t \leq \frac{\|\lambda\|_2^2}{\|\lambda\|_\infty}, \\ \exp\left(-\frac{t}{8\|\lambda\|_\infty}\right) & \text{if } t > \frac{\|\lambda\|_2^2}{\|\lambda\|_\infty}. \end{cases}$$

Let  $t = \|\lambda\|_1/2$ , then we have

$$\begin{aligned} \mathbb{P}\left(K_{ii} \leq \frac{1}{2m} \|\lambda\|_1\right) &\leq \max\left(\exp\left(-\frac{\|\lambda\|_1^2}{32\|\lambda\|_2^2}\right), \exp\left(-\frac{\|\lambda\|_1}{16\|\lambda\|_\infty}\right)\right) \\ &\stackrel{(a)}{\leq} \exp\left(-\frac{\|\lambda\|_1}{32\|\lambda\|_\infty}\right), \end{aligned}$$

where (a) holds due to Holder's inequality. Note that  $K_{TI,ii} = \max_{T \in \mathcal{G}} K_{linear}(TX_i, X_i) \geq K_{ii}, \forall i$ , then

$$\mathbb{P}(K_{TI,ii} \leq \frac{1}{2m} \|\lambda\|_1) \leq \mathbb{P}(K_{ii} \leq \frac{1}{2m} \|\lambda\|_1) \leq \exp\left(-\frac{\|\lambda\|_1}{32\|\lambda\|_\infty}\right). \quad (4)$$

Now we turn to the off-diagonal terms  $K_{TI,ij}$  for  $i \neq j$ . For  $p \in [m]$ , one can write

$$X_i^{(p)} X_j^{(p)} = (O \Lambda^{\frac{1}{2}} H_i)^T (O \Lambda^{\frac{1}{2}} H_j) = H_i^T \Lambda H_j = \sum_{p=1}^m \lambda^{(p)} H_i^{(p)} H_j^{(p)}.$$

Note that  $H_i^{(p)} H_j^{(p)} = \frac{1}{2}(Y_{+,ij}^{(p)} - Y_{-,ij}^{(p)})(Y_{+,ij}^{(p)} + Y_{-,ij}^{(p)})$ , where  $Y_{+,ij}^{(p)} := \frac{1}{\sqrt{2}}(X_j^{(p)} + X_i^{(p)})$  and  $Y_{-,ij}^{(p)} := \frac{1}{\sqrt{2}}(X_j^{(p)} - X_i^{(p)})$  are independent  $N(0, 1)$  random variables. Hence  $(Y_{+,ij}^{(p)})^2$  and  $(Y_{-,ij}^{(p)})^2$  are chi-squared random variables, and their moment generating functions are  $\mathbb{E}[e^{r(Y_{+,ij}^{(p)})^2}] = \mathbb{E}[e^{r(Y_{-,ij}^{(p)})^2}] = \frac{1}{\sqrt{1-2r}}$  for  $r < \frac{1}{2}$ . Hence for any  $|r| \leq 1/\|\lambda\|_\infty$ , we know

$$\begin{aligned} \mathbb{E}[e^{rX_i^\top X_j}] &= \mathbb{E}\left[\exp\left(r \sum_{p=1}^m \lambda^{(p)} H_i^{(p)} H_j^{(p)}\right)\right] = \mathbb{E}\left[\exp\left(\frac{r}{2} \sum_{p=1}^m \lambda^{(p)} \left((Y_{+,ij}^{(p)})^2 - (Y_{-,ij}^{(p)})^2\right)\right)\right] \\ &\stackrel{(b)}{=} \prod_{p=1}^m \mathbb{E}\left[\exp\left(\frac{r\lambda^{(p)}}{2}(Y_{+,ij}^{(p)})^2\right)\right] \mathbb{E}\left[\exp\left(-\frac{r\lambda^{(p)}}{2}(Y_{-,ij}^{(p)})^2\right)\right] \\ &= \prod_{p=1}^m \frac{1}{\sqrt{1 - (\lambda^{(p)})^2 r^2}}, \end{aligned}$$

where (b) is true since the random variables  $\{Y_{+,ij}^{(p)}, Y_{-,ij}^{(p)}\}_{p \in [m]}$  are mutually independent. It can be verified that  $\frac{1}{\sqrt{1-x}} \leq e^x$  for  $0 \leq x \leq 1/2$ . We can then upper bound the moment generating function of  $\mathbb{E}[e^{rX_i^\top X_j}]$ , since for any  $|r| \leq 1/\|\lambda\|_\infty$ ,

$$\mathbb{E}[e^{rX_i^\top X_j}] = \prod_{p=1}^m \frac{1}{\sqrt{1 - (\lambda^{(p)})^2 r^2}} \leq \prod_{p=1}^m \exp\left((\lambda^{(p)})^2 r^2\right) = \exp\left(\frac{2\|\lambda\|_2^2}{2} r^2\right).$$

This implies  $X_i^\top X_j \sim SE(\sqrt{2}\|\lambda\|_2, \|\lambda\|_\infty)$ . Since  $\mathbb{E}[X_i^\top X_j] = 0$ , by Lemma 4, we know

$$\mathbb{P}[X_i^\top X_j \geq t] \leq \begin{cases} \exp\left(-\frac{t^2}{4\|\lambda\|_2^2}\right) & \text{if } 0 \leq t \leq \frac{2\|\lambda\|_2^2}{\|\lambda\|_\infty}, \\ \exp\left(-\frac{t}{2\|\lambda\|_\infty}\right) & \text{if } t > \frac{2\|\lambda\|_2^2}{\|\lambda\|_\infty}. \end{cases}$$

Let  $t = \|\lambda\|_2(\ln m)^{(1+\epsilon)/2}$ . Under the assumption that  $\frac{\|\lambda\|_2}{\|\lambda\|_\infty} \geq \frac{(\ln m)^{(1+\epsilon)/2}}{2}$ , we have

$$\mathbb{P}\left[K_{ij} \geq \frac{\|\lambda\|_2(\ln m)^{\frac{1+\epsilon}{2}}}{m}\right] \leq \exp\left(-\frac{(\ln m)^{1+\epsilon}}{4}\right).$$

Note that  $|K_{TI,ij}| = |\sup_T K_{linear}(TX_i, X_j)| \leq \sup_T |K_{linear}(TX_i, X_j)|$ , then

$$\begin{aligned} \mathbb{P}(|K_{TI,ij}| \geq \frac{\|\lambda\|_2(\ln m)^{\frac{1+\epsilon}{2}}}{m}) &\leq \mathbb{P}(\sup_T |K_{linear}(TX_i, X_j)| \geq \frac{\|\lambda\|_2(\ln m)^{\frac{1+\epsilon}{2}}}{m}) \\ &\stackrel{(c)}{\leq} m\mathbb{P}(|K_{ij}| \geq \frac{\|\lambda\|_2(\ln m)^{\frac{1+\epsilon}{2}}}{m}) \stackrel{(d)}{\leq} 2m\mathbb{P}(K_{ij} \geq \frac{\|\lambda\|_2(\ln m)^{\frac{1+\epsilon}{2}}}{m}) \\ &\leq \exp\left(-\frac{(\ln m)^{1+\epsilon}}{4} + \ln 2m\right), \end{aligned} \quad (5)$$

where (c) holds since the distribution is translation invariant, and (d) holds since  $K_{ij}$  is a symmetric random variable, i.e.,  $p_{K_{ij}}(y) = p_{K_{ij}}(-y)$ .

Combining (4) and (5), we have

$$\begin{aligned} \mathbb{P}(K_{TI,ii} > \sum_{j \neq i} |K_{TI,ij}|, \forall i) &\geq \mathbb{P}(\min_i K_{TI,ii} > \max_i \sum_{j \neq i} |K_{TI,ij}|) \\ &\geq \mathbb{P}(\min_i K_{TI,ii} > \frac{\|\lambda\|_1}{2} \text{ and } \max_i \sum_{j \neq i} |K_{TI,ij}| < \frac{\|\lambda\|_2(\ln m)^{\frac{1+\epsilon}{2}} n}{m}) \end{aligned}$$

$$\begin{aligned}
&= 1 - \mathbb{P}(\min_i K_{TI,ii} \leq \frac{\|\lambda\|_1}{2} \text{ or } \max_i \sum_{j \neq i} |K_{TI,ij}| \geq \frac{\|\lambda\|_2(\ln m)^{\frac{1+\epsilon}{2}} n}{m}) \\
&\geq 1 - \mathbb{P}(\min_i K_{TI,ii} \leq \frac{\|\lambda\|_1}{2}) - \mathbb{P}(\max_i \sum_{j \neq i} |K_{TI,ij}| \geq \frac{\|\lambda\|_2(\ln m)^{\frac{1+\epsilon}{2}} n}{m}) \\
&= 1 - \mathbb{P}(K_{TI,ii} \leq \frac{\|\lambda\|_1}{2}, \exists i) - \mathbb{P}(\sum_{j \neq i} |K_{Ti,ij}| \geq \frac{\|\lambda\|_2(\ln m)^{\frac{1+\epsilon}{2}} n}{m}, \exists i) \\
&\stackrel{(e)}{\geq} 1 - n\mathbb{P}(K_{TI,ii} \leq \frac{\|\lambda\|_1}{2}) - n\mathbb{P}(|K_{Ti,ij}| \geq \frac{\|\lambda\|_2(\ln m)^{\frac{1+\epsilon}{2}} n}{m}, \exists j \neq i) \\
&\geq 1 - \exp(-\frac{\|\lambda\|_1}{32\|\lambda\|_\infty} + \ln n) - \exp(-\frac{1}{4}(\ln m)^{1+\epsilon} + 2\ln n + \ln 2m).
\end{aligned}$$

Above, (e) holds since the probability distributions of  $|K_{TI,ij}|$  are identical for all  $j \neq i$ . Since  $\|\lambda\|_1 \geq \|\lambda\|_2$ , the assumption  $\frac{\|\lambda\|_2}{\|\lambda\|_\infty} \geq (\ln m)^{(1+\epsilon)/2}$  implies  $\frac{\|\lambda\|_1}{\|\lambda\|_\infty} \geq (\ln m)^{(1+\epsilon)/2}$ . Note that  $n = \tilde{O}(\sqrt{m})$ , then

$$\lim_{m \rightarrow \infty} \mathbb{P}(K_{TI,ii} > \sum_{j \neq i} |K_{TI,ij}|, \forall i) \geq \lim_{m \rightarrow \infty} 1 - \frac{1}{\text{poly}(m)} = 1.$$

Therefore,  $K_{TI,best,linear}$  is a positive definite kernel with probability approaching one as  $m \rightarrow \infty$ .  $\square$